Highly Fluorescent Crystalline and Liquid Crystalline Columnar Phases of Pyrene-Based Structures

Anna Hayer,[⊥] Véronique de Halleux,[‡] Anna Köhler,[⊥,||] Abdel El-Garoughy,[†] E. W. Meijer,[†] Joaquín Barberá,[§] Julien Tant,[‡] Jeremy Levin,[‡] Matthias Lehmann,[‡,¶] Johannes Gierschner,[#] Jérôme Cornil,[#] and Yves Henri Geerts*[,‡]

Laboratoire de chimie des polymères, CP 206/1, Université Libre de Bruxelles, Boulevard du Triomphe, 1050 Bruxelles, Belgium, Cavendish Laboratory, Department of Physics, University of Cambridge, Madingley Road, Cambridge CB3 0HE, United Kingdom, Institute of Physics, University of Potsdam, Am Neuen Palais 10, 14469 Potsdam, Germany, Laboratory of Macromolecular and Organic Chemistry, Eindhoven University of Technology, P.O. Box 513, 5600 MB Eindhoven, The Netherlands, Química Orgánica, Facultad de Ciencias-I.C.M.A., Universidad de Zaragoza-C.S.I.C., 50009-Zaragoza, Spain, Institute of Chemistry, Chemnitz University of Technology, Strasse der Nationen 62, 09111 Chemnitz, Germany, and Laboratory for Chemistry of Novel Materials, University of Mons-Hainaut, Place du Parc 20, 7000 Mons, Belgium

Received: December 17, 2005; In Final Form: March 4, 2006

A concept for highly ordered solid-state structures with bright fluorescence is proposed: liquid crystals based on tetraethynylpyrene chromophores, where the rigid core is functionalized with flexible, promesogenic alkoxy chains. The synthesis of this novel material is presented. The thermotropic properties are studied by means of differential scanning calorimetry (DSC), cross-polarized optical microscopy (POM), and X-ray diffraction. The mesogen possesses an enantiotropic Col_h phase over a large temperature range before clearing. The material is highly fluorescent in solution and, most remarkably, in the condensed state, with a broad, strongly red shifted emission. Fluorescence quantum yields (Φ_F) have been determined to be 70% in dichloromethane solution and 62% in the solid state. Concentration- and temperature-dependent absorption and emission studies as well as quantum-chemical calculations on isolated molecules and dimers are used to clarify the type of intermolecular interactions present as well as their influence on the fluorescence quantum yield and spectral properties of the material. The high luminescence efficiency in the solid state is ascribed to rotated chromophores, leading to an optically allowed lowest optical transition.

Introduction

Discotic liquid crystals (LC) possess the ability to self-organize into highly anisotropic and ordered structures such as columns.[1] If this is combined with suitable optical and electronic properties, this results in ideal building blocks for smart materials in optoelectronic devices. However, the intermolecular interactions responsible for self-organization can also have a dramatic influence on the electrical and photophysical properties of molecules such as spectral characteristics, energy transfer, charge generation and transfer, excitation decay pathways, and luminescence efficiency. A thorough understanding of the types of intermolecular interactions occurring and of their physical effects is therefore needed for the rational design of novel materials for optoelectronic applications.

One potential application is the transport of excitation energy over large distances. Discotic LCs would be ideal candidates since in addition to self-organization into highly anisotropic structures, they tend to eliminate structural and electronic defects by self-healing[2] and have a fluidity that allows for easy film preparation. However, up to now, energy transfer has been mostly studied in weakly fluorescent discotic LC.[3] We postulate that the combination of columnar stacking of discotic aromatic molecules and high fluorescence should be beneficial for energy transfer since the Förster mechanism should become more effective. Only a few highly fluorescent discotic LC forming columnar phases have been synthesized so far.[2,4−6]

There are often strong interchromophoric interactions associated with the formation of LC stacks. In many cases, such interactions (such as aggregate and excimer formation) are detrimental to the fluorescence efficiency. Consequently, to promote strong emission from LCs, one would need either to form stacks without interchromophoric interactions (which may be extremely difficult to achieve) or find systems where these interactions do not quench the fluorescence. Pyrene is known to have a high fluorescence quantum yield in solution[7] but also to show efficient excimer emission.[8,9] Furthermore, pyrene offers the advantage of being easily functionalized at the 1, 3, 6, and 8 positions. Initial studies for incorporating a pyrene core into LCs have been presented.[6b,e] However, the nature of the specific interchromophoric interactions in the solid state and the quantum yields were not studied in detail. Recently, we reported the synthesis of tetraphenylpyrene derivatives that were all strongly emitting in solution and in the solid state but did not form any columnar mesophase. This has been attributed to the steric hindrance associated to the four orthogonal phenyl substituents that prevents the close stacking of the pyrene cores.[10,11] To

* Address correspondence to this author. E-mail: ygeerts@ulb.ac.be.
[⊥] University of Cambridge.
[‡] Université Libre de Bruxelles.
[||] University of Potsdam.
[†] Eindhoven University of Technology.
[§] Universidad de Zaragoza-C.S.I.C.
[¶] Chemnitz University of Technology.
[#] University of Mons-Hainaut.

10.1021/jp0573689 CCC: $30.25
Published on Web 03/29/2006

SCHEME 1: Synthesis of TDPEPy (3) by the Sonigashira-Hagihara Reaction

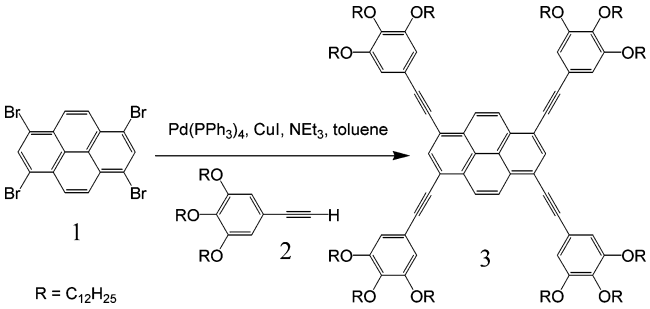

obtain the combination of intense fluorescence and columnar mesophase, we have substituted the flat tetraethynylpyrene unit with promesogenic side groups.[11] These side groups should have a high tendency to induce a liquid crystalline behavior.

In the present work, we describe the design of a new discotic mesogen based on the tetraethynylpyrene core (Scheme 1): 1,3,6,8-tetrakis(3,4,5-trisdodecyloxyphenylethynyl)pyrene (TDPEPy). It forms columnar liquid crystal phases over a substantial temperature range. Moreover, this molecule exhibits a strong luminescence in solution, in the crystal and liquid crystalline states. The type of intermolecular interactions present as well as their influence on the fluorescence quantum yield and spectral properties are probed by a combined experimental and theoretical study including concentration- and temperature-dependent absorption and emission spectra in solutions and films and quantum-chemical calculations on individual molecules and dimers.

Results and Discussion

Synthesis and Characterization. To allow for further experimental characterizations, functional liquid crystals should be available in large amounts of pure analytical products. Synthetic schemes must involve a few reaction steps with high yields and easy purification procedures. The target molecule TDPEPy (**3**) has been prepared by a convergent synthesis, using the pyrene derivative **1** as the connecting core. Following this strategy, TDPEPy (**3**) has been obtained in 35% yield, by coupling 3,4,5-tridodecyloxyphenylacetylene (**2**)[12] to 1,3,6,8-tetrabromopyrene (**1**),[13] using Sonigashira−Hagihara's method[14] (Scheme 1). The structure and purity of TDPEPy (**3**) were verified by ^{1}H and ^{13}C NMR spectroscopy, field desorption (FD) mass spectrometry, and elemental analysis. The symmetric substitution on the central chromophore is evidenced by two singlets in the ^{1}H NMR spectra at δ 8.73 and 8.42 ppm associated to four and two protons, respectively. These protons can be easily distinguished from the signal of the eight aromatic protons at δ 6.90 ppm attributed to the substituted peripheral phenyl rings. No asymmetrically substituted products have been detected either by NMR or by FD mass spectroscopy.

Thermotropic Behavior. The thermotropic behavior of TDPEPy has been investigated by means of differential scanning calorimetry (DSC) and cross-polarized optical microscopy (POM). Additional characterizations of the mesophases and the determination of the structural parameters have been performed by powder X-ray diffraction. The DSC trace of TDPEPy shows two first-order phase transitions upon heating and three transitions upon cooling from the isotropic phase (Table 1). POM reveals fluid and birefringent mesophases between 52 and 95 °C upon heating and from 90 to 38 °C upon cooling. Furthermore, upon slow cooling from the isotropic liquid phase, digitated stars can be observed (Figure 1), which are typically of hexagonal columnar mesophases.[15]

TABLE 1: Thermal Behavior of TDPEPy Investigated by DSC[a]

	T [°C]/ΔH [kJ mol^{-1}] rate 10 °C/min
2nd heating	Cr 51.5/28.3 Col_h 95.5/3.8 I
1st cooling	I 90.0/−3.2 Col_h 50.0/−5.0 Col_r 38.5/−16.0 Cr

[a] Cr crystalline phase, Col_h columnar hexagonal phase, Col_r columnar rectangular phase, I = isotropic liquid phase.

The transition between the isotropic and LC phase shows a small temperature hysteresis and a transition enthalpy value typical for columnar liquid crystalline phases (see Table 1). The transitions at 51.5 °C (upon heating) and 38.5 °C (upon cooling) display a large hysteresis and enthalpies consistent with Cr-LC transitions. A third transition with a small enthalpy of 5.0 kJ/mol at 50 °C is found only in the cooling trace and is assigned to a LC-LC transition. Thus, the low-temperature mesophase is monotropic, i.e., a metastable phase that appears only upon cooling, contrary to the high-temperature mesophase which is enantiotropic, i.e., a stable phase that appears during both the heating and cooling cycles. To obtain more insight into the nature of the various phases, powder X-ray diffractograms have been taken. The diffraction photographs taken at room temperature unambiguously indicate the 3D-crystalline nature of the virgin powder as well as that of the solid crystallized from the high-temperature phase. This is demonstrated by the presence of sharp reflections in all angular regions. On the other hand, at high temperatures, the patterns are characteristic of mesomorphic phases, as shown by the absence of reflections in the middle and wide-angle regions and the presence of reflections only at small angles and of a diffuse halo at wide angles. The X-ray patterns taken with a sample cooled to 40 °C display a strong reflection corresponding to a spacing of 33.5 Å and a set of weak reflections (Table 2). These reflections can be assigned to a rectangular lattice. The two-dimensional character is confirmed by the absence of reflections with the third Miller index l different from zero. For all reflections, $h + k = 2n$ (with n an integer number), which indicates that the lattice is centered on the AB plane and is thus a C-centered orthorhombic lattice. All these features are consistent with a rectangular columnar mesophase (Col_r) with a $c2mm$ symmetry.[16] In this mesophase, each disklike molecule stacks on top of another and the columns generated adopt a rectangular packing with the columnar axes located at the corners and at the center of the rectangle. The disks are tilted versus the columnar axis by an angle α (Scheme 2) that could not be determined from the present diffraction data. The disk projection in the plane perpendicular to the columnar axis thus appears ellipsoid shaped (Scheme 2). A distance of $c \sim 4.4$ Å separates the aromatic planes

At 60 °C, the diffraction photographs display a single reflection at 32.6 Å, in addition to the broad halo at 4.6 Å (Table 2). Although the presence of a single maximum at low angles does not allow for an unambiguous determination of the mesophase structure, the microscope textures are consistent with a uniaxial, hexagonal columnar structure (Col_h). The absence of other reflections apart from the (100) reflection is frequent in diffraction patterns of hexagonal columnar mesophases;[17] it is due to a minimum in the form factor, which precludes the observation of peaks in this angular region. To exclude the formation of the rarely observed uniaxial square columnar mesophase, the diameter of a model for the columnar packing based on microsegregated core and aliphatic chains can be estimated for the square and hexagonal phases and compared to the experimental value. The creation of a model starts with

Figure 1. Optical micrographs of TDPEPy: digitate stars observed in the mesophase at 88 °C upon cooling from the isotropic phase (left) and hexagonal growing nonbirefringent germ between parallel polarizers (right).[23b]

TABLE 2: X-ray Diffraction Data for TDPEPy

temp, °C	phase	*hkl*	d_{obs} (Å)	d_{calc} (Å)	lattice constants (Å)
40	Col_r	200	33.5	33.5	$a = 67.0$
	mesophase	310	18.3	18.5	$b = 33.0$
		400	16.8	16.75	
		510	12.4	12.4	
		130	10.6	10.85	
		330	10.0	9.9	
		530	8.7	8.5	
		240	7.9	8.0	
		440	7.4	7.4	
			4.4[a]		$c \sim 4.4$
60	Col_h	100	32.6	32.6	$a = 37.6$
	mesophase		4.6[a]		$c \sim 4.6$

[a] Diffuse maximum.

SCHEME 2: Schematic Drawing of (1) the Col_r Mesophase with a *c2mm* Symmetry and (2) the Col_h Mesophase

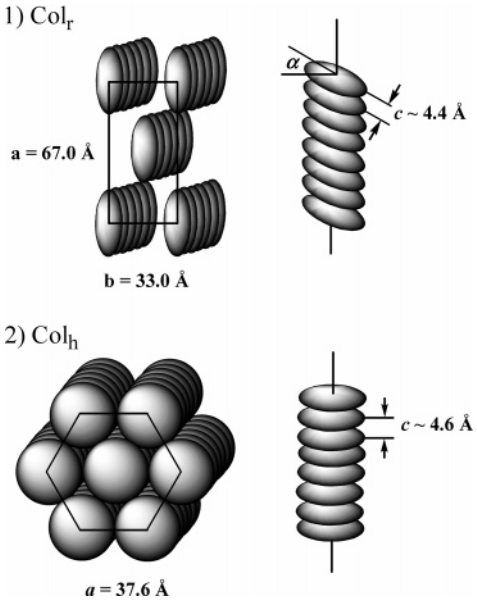

the estimation of the number of molecules filling a columnar slice of heigth $h = 4.6$ Å, which is the building block of the columns.[18] The number of molecules can be obtained as $Z = \delta \times N_A \times V_{unitcell}/M$, assuming a density $\delta = 1$ g/cm^3 for the organic material, with $M = 2818.6$ g/mol the molecular mass, N_A Avogadro's constant, and $V_{unitcell}$ the volume of the unit cell. $V_{unitcell}$ can be calculated from the measured parameters (Table 2), taking into account the phase geometry. For the hexagonal phase $V_{unitcellhex} = a_{hex}^2 \times \sin 60 \times h = 5632$ Å^3 (unit cell parameter of the hexagonal phase: $a_{hex} = 37.6$ Å with $h = 4.6$ Å), while for the square phase $V_{unitcellsquare} = a_{sq}^2 \times h = 4889$ Å^3 (unit cell parameter of the square phase: $a_{sq} = 32.6$ Å with $h = 4.6$ Å). The corresponding number of molecules per unit cell amounts to $Z_{sq} = 1.04$ and $Z_{hex} = 1.20$ for the square and hexagonal columnar phases, respectively. The building block for the columns, which fills the space of a columnar slice, is thus represented by approximately one molecule in both cases. A molecule consists of the core and 12 peripheral aliphatic chains. The volume filled by the aliphatic chains at a given temperature T can be calculated by using volume fractions of CH_2 and CH_3 groups obtained from dilatometry studies.[18] The volume of the 12 dodecyloxy chains at $T = 60$ °C in the LC phase is estimated to be $V_{chain} = 4022.4$ Å^3. The difference between the volume of the unit cell and the volume of the chains yields the volume occupied by the aromatic core unit ($V_{core} = V_{unit\ cell} - V_{chain}$). Since the cross section for the aromatic cores should be circular in a unixial phase, the radius of the core in this phase geometry can be estimated by $r = V_{core}^{1/2}/(\pi \times h)$. With the assumption of one molecule in the unit cell, radii $r_{sq} = 7.7$ Å and $r_{hex} = 12.4$ Å are obtained for the square and hexagonal columnar phases, respectively. The core radius of 10.88 Å estimated from the geometry optimized at the semiempirical Hartree−Fock AM1 (Austin Model 1) level as the distance between the center of the core to the oxygen of an alkoxy chain in the para position compares well with the results obtained for the hexagonal phase. These considerations support the model of a hexagonal phase formed by microsegregation of the aliphatic and aromatic subunits of TDPEPy. Thus, TDPEPy self-organizes into an enantiotropic Col_h and a monotropic Col_r phase. The mesomorphic behavior is generated by the anisotropic molecular shape as well as by the microsegregation of the 12 long aliphatic side chains pointing away from the rigid 1,3,6,8-tetraphenylethynylpyrene core.

Photophysical Properties. *Dilute Solutions.* Absorption and emission spectra of TDPEPy have been taken in dilute dichloromethane solutions (Figure 2). The main absorption band peaks at 2.58 eV (481 nm; $\epsilon = 66\,000$ L mol^{-1} cm^{-1}) and shows a vibronic replica at 2.73 eV (454 nm; $\epsilon = 51\,000$ L mol^{-1} cm^{-1}). The emission spectrum with its 0−0 transition at 2.47 eV (502 nm) and its 0−1 transition at 2.31 eV (537 nm) is a good approximation of the mirror image of the absorption. The strong bathochromic shift compared to pyrene exhibiting a 0−0 transition of fluorescence at around 420 nm = 2.95 eV[8] suggests a significantly increased effective chromophore size in TDPEPy. This implies that the ethynyl side chains and the lateral alkoxy-substituted phenyl groups contribute substantially to the conjugated system. The conformational disorder induced by the phenyl groups contributes to the line broadening in TDPEPy.

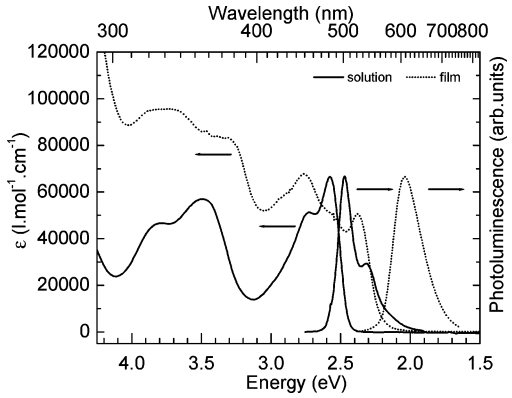

Figure 2. Absorption and emission spectra of TDPEPy at 1×10^{-5} mol/L of solution in CH_2Cl_2 and in thin film taken at room temperature.

Quantum-chemical calculations performed at the ZINDO/S level show that the lowest vertical transition (S_1) of the model compound tetra(phenylethynyl)pyrene (without the alkoxy side chains) is strongly optically allowed, with an oscillator strength f of 1.61. It is located at $E_{max} = 2.80$ eV, in quite good agreement with the experimental value. A second state is found 0.28 eV above S_1 with $f = 0.03$. This is probably the main reason for the somewhat enhanced broadening of the absorption spectrum. Including 12 methoxy substituents to account for the effect of alkoxy substitution further decreases the calculated transition energies to 2.78 ($f = 1.65$) and 3.08 eV ($f = 0.04$).

The fact that the lowest optical transition is strongly allowed in TDPEPy constitutes a major difference compared to unsubstituted pyrene where the lowest transition is only weakly allowed according to both experimental[19] and theoretical[20] studies. The large oscillator strength of the lowest transition is consistent with the remarkably high fluorescence quantum yield observed in solution. At 10^{-5} mol/L in dichloromethane, a fluorescence quantum yield (Φ_F) of 70 ± 5% is measured for TDPEPy under 457 nm excitation, using Rhodamine 6G as the standard.

Concentrated Solutions. Figure 3a shows the concentration dependence of the emission spectra of TDPEPy. At concentrations larger than 10^{-6} mol/L, self-absorption starts to reduce the intensity of the highest energy peak but the spectral shape is otherwise unaffected up to 10^{-3} mol/L, indicating that only intrinsic intramolecular emission is detected. At 10^{-2} mol/L, an additional broad and unstructured shoulder appears in the spectrum. It becomes the dominant spectral feature above 1.5×10^{-2} mol/L and peaks at around 2 eV. This emission is attributed to excimer formation, thus implying that the interaction occurs only in the excited state, for the following reasons. No attractive interactions take place in solution between molecules in the ground state, as evidenced by concentration-independent ^{1}H chemical shift of aromatic protons from 10^{-4} mol/L to 10^{-2} mol/L in deuterated chloroform solution. This is further corroborated by the evolution of the absorption spectra as a function of the concentration (Figure 3b). Even at concentrations above 10^{-2} mol/L at which the broad and unstructured intermolecular features dominate the emission spectrum, no additional absorption bands are observed, though the inhomogeneous broadening of the absorption bands is found to increase.

Pyrene is well-known for its tendency to form highly luminescent excimers. In fact, excimer fluorescence from aromatic hydrocarbons was first identified by Förster and Kasper when studying solutions of pyrene of increasing concentration by the observation of a broad, red-shifted emission for concentrations above 10^{-3} mol/L.[8] The excimer observed in the present study is also formed by stacking pyrene cores; the fact that the emission is significantly red-shifted with respect to the excimer emission for pyrene itself (around 480 nm = 2.58 eV) suggests that the ethynyl side chains and the lateral alkoxy-substituted phenyl groups are also in interaction.

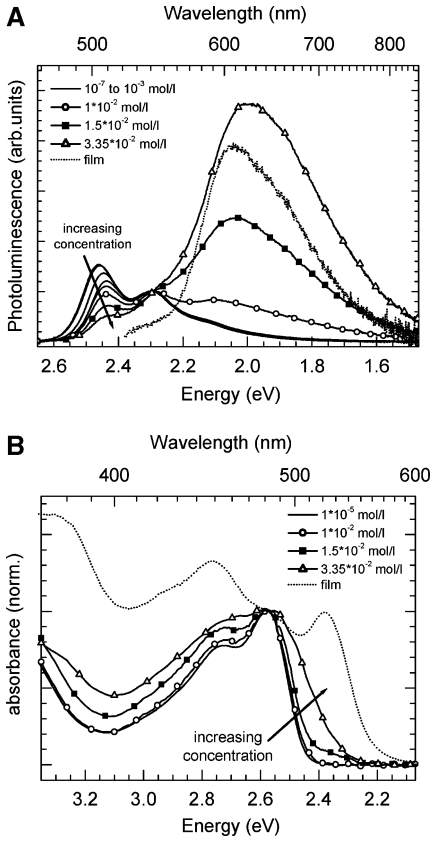

Figure 3. Concentration-dependent emission (panel A) and absorption (panel B) spectra of TDPEPy in CH_2Cl_2.

Thin Films. Room-temperature absorption and emission spectra of thin crystalline films of TDPEPy drop-cast from solution are shown in Figure 2 (dotted lines). In the film, both the absorption and emission spectra are broader and much less resolved than in solution. The absorption spectrum displays two peaks at 2.76 (449 nm) and 2.36 eV (522 nm), in contrast to the single feature observed at 2.58 eV (481 nm) in solution. The fluorescence spectrum is strongly red-shifted and structureless with a maximum at 2.04 eV (607 nm). It closely resembles the excimer fluorescence of TDPEPy in concentrated solutions (Figure 3a). A strong fluorescence is observed in the different solid-state phases at different temperatures following irradiation at 354 nm. A quantum yield of 62 ± 6% has been determined in the film at room temperature under UV excitation by using the integrating sphere technique.[21] This efficiency in the solid state is comparable to that of polymers such as polyfluorene (55%)[22] and polyparaphenylenevinylene (PPV) derivatives (33%).[23] To the best of our knowledge, these values are among the highest fluorescence quantum yields reported so far for discotics. We attribute this unusually high efficiency to the excimer-like solid-state emission resulting from the particular molecular arrangement of TDPEPy in the solid state that we deduce hereafter.

Figure 4 shows the absorption spectra at 73 °C in the liquid crystalline phase (top) and at 20 °C in the crystalline phase (bottom). In the liquid crystalline phase, the spectrum displays two peaks at 2.39 (519 nm) and 2.60 eV (477 nm) and a

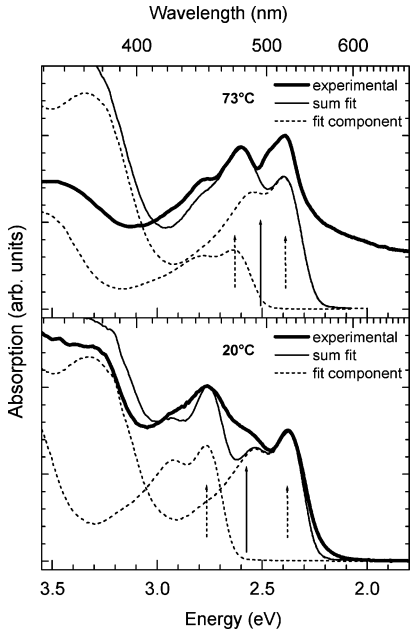

Figure 4. Absorption spectra in thin films at 73 °C (top) and room temperature (bottom) fitted as a superposition of shifted solution spectra. The dashed arrows mark the peak positions of the individual fit components, solid arrows mark the center of this splitting.

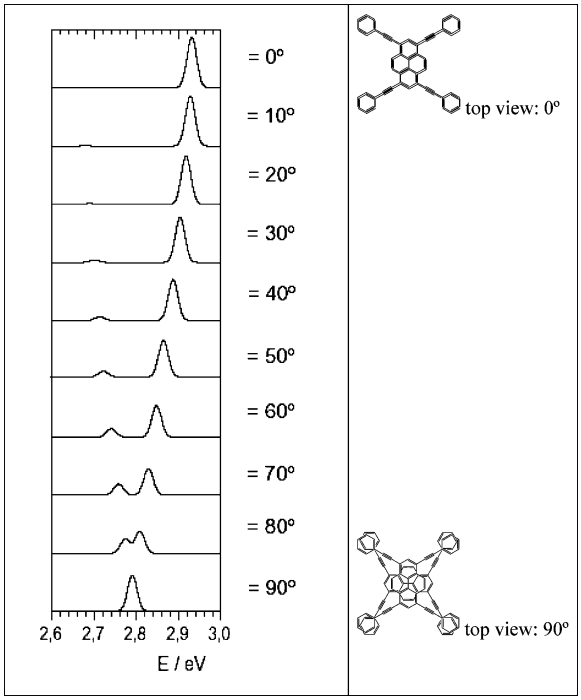

Figure 5. Calculated spectral positions and relative intensities of the $S_0 \rightarrow S_1$ and $S_0 \rightarrow S_2$ dimer absorption bands of a cofacial TPEPy pair (separation 4.6 Å) as a function of the rotation angle. The absorption bands are depicted as Gaussians.

shoulder around 2.78 eV (446 nm). (The low energy tail of the spectrum extends linearly into the red spectral range even below the emission and is therefore attributed to scattering.) In the crystalline phase, the lower energy peak is slightly red-shifted to 2.38 eV (521 nm) while the higher energy peak is blue-shifted to 2.76 eV (449 nm). The fact that the absorption spectra in both solid phases are very different from that in solution (Figure 2) points toward significant ground-state interactions in the solid state, in agreement with the formation of a crystalline phase at room temperature. To uncover the nature of the species observed in the solid state, quantum-chemical calculations have been carried out on cofacial dimers made of tetra(phenylethynyl)-pyrene (TPEPy) as a simplified model for stacks containing more than two molecular units. The absorption at room temperature cannot be modeled directly because the exact interchromophoric distance is unknown. We have thus focused on the hexagonal liquid crystalline phase in which the interchromophoric distance is estimated to be $c \sim 4.6$ Å and the stacking direction is perpendicular to the molecular plane. For such an intermolecular distance, the interaction between the S_0-S_1 transition dipole moments is in the medium coupling regime and leads to a symmetric splitting into two states S_1', S_2', with the lower S_1' state forbidden for a parallel orientation of the two molecules, see Figure 5. The mutual rotation of the two monomers determines not only the extent of the splitting but also the relative intensity of the two subbands:[24] progressive deviation from the co-parallel orientation leads to a growing increase in the intensity of the S_1' state. Although the overall optical splitting is expected to be smaller in a dimer than in larger stacks, this simple approach already yields a correct qualitative picture. These results show that the experimental absorption spectrum of the liquid crystalline phase can be rationalized by an arrangement in the stacks with the molecules rotated by about 70−80°. Such a rotation reduces the steric interactions between the substituents compared to an arrangement at 0° or 90°. The large oscillator strength of the lower energy component explains why emission is strongly allowed in the stacks and why a high fluorescence quantum yield is obtained. A high solid-state luminescence efficiency resulting from a cross-like dipolar stacking has also been reported recently for the crystalline distyrylbenzene derivative.[25]

In agreement with a two-state model, the absorption spectrum taken in the liquid-crystalline phase at 73 °C can be roughly fitted as a superposition of two solution spectra which are broadened by 10% (Figure 4, top). (The scattering mentioned above leads to an apparent intensity mismatch of the lowest absorption peak between the experimental and fitted spectra.) The observed splitting in the LC phase of ca. 240 meV is larger than the value of 30−70 meV calculated for a dimer since the optical splitting grows with the number of molecules in the stack. The absorption spectrum of the crystalline thin film at room temperature can also be qualitatively understood by applying the two-state model. The bottom part of Figure 4 shows a comparison between the experimental spectrum in the crystalline phase and a superposition of two shifted solution spectra. The splitting of ca. 310 meV is larger than that in the liquid-crystalline phase, as expected due to the shorter distances between the molecules and thus stronger intermolecular interactions in the crystal.

The increase in the ground-state interaction going from the concentrated solution to the crystal is due both to the enthalpy gained by the close packing in the solid state and to the fact that electrostatic forces such as van der Waals interactions can modify the ground state potential so that it becomes fairly flat or even weakly attractive. As a result, the molecules are coerced into close contact configurations which allow for the creation of collective excitations (i.e., delocalized over several molecules). This behavior is similar to that observed for pyrene itself: although the absorption spectrum of a pyrene crystal is relatively well-structured,[26] and similar to the absorption spectrum in solution, the absorption edge in the crystal is red-shifted against the solution, indicating some interchromophore interactions.[27−30] In the excited state of the pyrene[31] and TDPEPy crystals, the intermolecular interactions are expected to become more attractive,[32,33] leading to emission features very

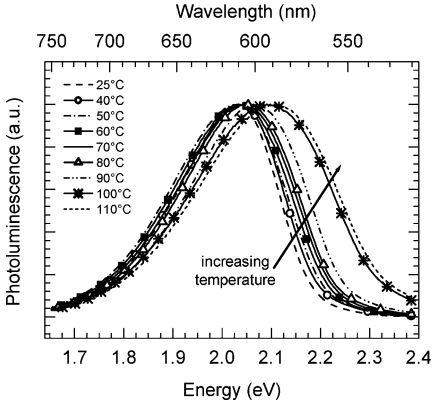

Figure 6. Temperature-dependent emission spectra of TDPEPy in thin films upon heating.

similar to the excimer emission in concentrated solutions. According to Birks,[34] these systems should also be called excimers, redefined as "a molecular dimer or stoichiometric complex which is associated in an excited electronic state and which is *dissociative* (*i.e.*, dissociates in the absence of external restraints) in its electronic ground state". The origin of the unstructured, strongly red-shifted emission can therefore be seen in the substantial decrease in the intermolecular separation upon excitation, which enables a very efficient coupling of low-frequency intermolecular breathing modes to the electronic transition responsible for the loss of spectral resolution.[32,33]

When the temperature is increased, the thin film emission spectrum is blue-shifted, owing to the decrease in the amplitude of the stabilizing intermolecular interactions when the interchromophore distances get larger (Figure 6). However, this shift does not evolve monotically: below 90 °C, i.e. the transition to the isotropic phase, there is a small continuous blue-shift resulting from the decrease in density of the material as the molecules are slowly pulled apart. The phase transition from the crystalline to the hexagonal liquid-crystalline phase does not have a strong influence on the emission spectrum since this affects primarily the interstack ordering rather than the interchromophoric distances within the stacks. At 90 °C, there is a strong sudden change in emission at the phase transition from the liquid-crystalline to the isotropic phase. At this transition, large stacks may break up, thus reducing the interchromophoric interactions to lead to a considerable blue-shift of the emission. However, small stacks made of a few chromophores should still persist due to the favorable packing effects. Such local stackings of discotic cores well above the clearing point has been reported previously.[35,36] This rationalizes why the emission of the isotropic phase is still at much lower energy than that observed in solution (2.1 eV vs 2.47 eV) and does not exhibit resolved vibronic features.

Conclusions

We have reported the synthesis of a new tetrakis(trisalkoxyphenylethynyl)pyrene discotic mesogen that forms hexagonal and rectangular columnar mesophases. In addition to a high fluorescence quantum yield in solution, this molecule exhibits a quantum yield in the crystalline phase as high as $62 \pm 6\%$. To the best of our knowledge, this value is one of the highest fluorescence quantum yields reported so far for discotics. This high efficiency coupled to the columnar arrangement generated upon self-assembly might prove beneficial in optoelectronic applications, for example, for excitation energy transfer over large distances.

Concentration-dependent studies show excimer-type emission at high concentration in solution. The absorption and emission characteristics measured for the different solid phases at various temperatures point to the formation of cofacial stacks with the chromophores rotated by 70−80°; this picture is fully supported by the results of quantum-chemical calculations. This mutual rotation of the chromophores promotes an optically allowed lowest excited state for aggregated molecule species which is at the origin of the high fluorescence quantum yield. An excimer-type emission very similar to that prevailing in concentrated solutions is observed in the solid state. In contrast, the stacks in the solid state show considerable ground-state interactions, resulting in a significantly modified absorption spectrum compared to those in concentrated solutions. The emitting species in the solid state is classified as a "solid-state excimer" following the definition of Birks,[34] namely a dimer with a *dissociative*, but not necessarily dissociated, ground state.

Experimental Section

The thermal behavior of all the materials synthesized was investigated by polarizing optical microscopy (JENA microscope equipped with a Mettler FP 52 hot stage and a Zeiss Axioskop 40 A with a Linkam temperature controller (TP 94)) and differential scanning calorimetry (Mettler Toledo DSC 821, 3−9 mg samples in closed Al pans) with heating and cooling scans performed at 10 °C min^{-1} unless stated otherwise (peak values are given). X-ray diffraction patterns were obtained with a pinhole camera (Anton-Paar) operating with a point-focused, Ni-filtered Cu Kα beam. The samples were held in Lindemann glass capillaries (1 mm diameter) and heated with a variable-temperature attachment. The X-ray patterns were collected on flat photographic film, located at different distances from the sample depending on the angular region to explore. ^{1}H NMR spectra were recorded in $CDCl_3$, $C_2D_2Cl_4$, and DMSO-d_6 as solvents on a Bruker Avance 300, Bruker AC 250, and Varian Unity 600 (600 MHz) with solvent signal as the internal standard. Mass spectra were recorded on a VG Micromass 7070F instrument (electron impact, 70 eV) and a VG analytical ZAB 2-SE-FPD: FD (8 kV). Elemental analyses were carried out with a Perkin-Elmer 240.

Thin solid films have been obtained by either drop casting from dichloromethane solutions of the corresponding compounds onto CaF_2 pellets or spin-coating onto quartz substrates. Solvents and reagents were purchased from Aldrich and used as received. The solvents for the photophysical study were of spectroscopic grade and were used as received. Column chromatographies were performed on silica gel (Merck silica gel 60, mesh size 0.2−0.5 mm).

UV/vis absorption measurements at room temperature were performed with a HP 8453 spectrophotometer. At high temperature, samples were placed in a vacuum chamber and a probe beam generated by a 150 W tungsten halogen lamp and monochromated with two Chromex 250SM scanning monochromators (before and after the sample) was detected by a Si photodiode coupled to a SR830 dual phase lock-in amplifier. Temperature-dependent emission measurements were carried out with a SLM-Aminco 3000 diode array spectrophotometer. Concentration-dependent emission spectra were obtained with a spectrograph and cooled charge coupled device (CCD) array (Oriel instaspec) under excitation with the 351 and 364 nm lines of an Ar ion laser. The same detection setup was coupled to an integrating sphere via an optical fiber to obtain quantum yields of fluorescence.[32] The sphere was continuously purged with nitrogen.

Semiempirical quantum-chemical calculations have been performed on the isolated molecules and dimers for the unsubstituted (TPEPy) and methoxy-substituted tetra(phenylethynyl)pyrenemolecules. The geometries of the molecules were optimized at the Hartree−Fock Austin Model 1 (AM1)[37] level; vertical electronic transition energies were calculated with the ZINDO/S method (Intermediate Neglect of Differential Overlap method, as parametrized by Zerner and co-workers, coupled to a Single Configuration Interaction scheme),[38] with an active space encompassing all the occupied/unoccupied π-orbitals.

1,3,6,8-Tetrakis(3,4,5-trisdodecyloxyphenylethynyl)-pyrene (3). Dry triethylamine (75 mL) was added to a solution of tetrabromopyrene **1** (79 mg, 0.15 mmol) in 75 mL of dry toluene in a Schlenk flask. The flask was evacuated and flushed with nitrogen several times. An excess of alkyne **2** (500 mg, 0.76 mmol, 5 equiv), $Pd(PPh_3)_4$ (8 mol %, 14 mg, 0.012 mmol), and CuI (10 mol %, 3 mg, 0.015 mmol) were added. The flask was evacuated and flushed with nitrogen three times. After stirring, under nitrogen atmosphere for 24 h at 80 °C, the reaction mixture was poured into a 3-fold volume of ice/HCl 37 wt % in water (3:1) and the aqueous phase extracted with CH_2Cl_2. The organic layer was dried with $MgSO_4$ and the solvent was evaporated. The crude product was purified twice by column chromatography on silica, first with hexane:dichloromethane (8:2) as solvent and second with hexane, to give 148 mg (35%) of the title compound as an orange solid, mp 52 °C, clearing point 96 °C. ^{1}H NMR (300 MHz, $CDCl_3$) δ 8.73 (s, 4H, ArH), 8.42 (s, 2H, ArH), 6.90 (s, 8H, ArH), 4.03 (m, 24H, α-CH_2), 1.82 (m, 24H, CH_2), 1.54−1.31 (m, 216H, CH_2), 0.86 (m, 36H, CH_3); ^{13}C NMR (75 MHz, $CDCl_3$) δ 153.9, 140.3, 134.4, 132.3, 127.5, 124.9, 119.7, 118.2, 111.0, 97.2, 87.1, 74.3, 70.0, 32.6, 31.1, 30.3, 30.1, 26.8, 23.4, 14.8; MS (MALDI-TOF) *m*/*z* (%) 2814 (M^+, 100%). Elemental Anal. calcd for $C_{192}H_{314}O_{12}$: C 81.93, H 11.24. Found: C 82.00, H 11.38.

Acknowledgment. This work was financially supported by the Belgian National Science Foundation (FNRS- FRFC no. 2.4608.04, FNRS "crédit aux chercheurs" no. 1.5.074.00), Université Libre de Bruxelles, Banque Nationale de Belgique, Communauté Française de Belgique (ARC no. 00/05-257), and European Union (DISCEL G5RD-CT-2000-00321). V.d.H. and J.T. acknowledge FRIA for a fellowship. A.K. thanks the Royal Society and Peterhouse for financial support. J.C. is a FNRS research fellow.

References and Notes

(1) For a brief review of discotics see: Chandrasekhar, S. *Liq. Cryst.* **1993**, *14*, 3 and references therein.

(2) (a) Cormier, R. A.; Gregg, B. A. *J. Phys. Chem. B* **1997**, *101*, 11004−11006. (b) Cormier, R. A.; Gregg, B. A. *Chem. Mater.* **1998**, *10*, 1309−1319.

(3) Marguet, S.; Markovitsi, D.; Millié, P.; Sigal, H.; Kumar, S. *J. Phys. Chem. B* **1998**, *102*, 4697−4710.

(4) Rohr, U.; Schlichting, P.; Böhm, A.; Gross, M.; Meerholz, K.; Bräuchle, C.; Müllen, K. *Angew. Chem., Int. Ed.* **1998**, *37*, 10, 1434−1437.

(5) (a) Sautter, A.; Thalacker, C.; Würthner, F. *Angew. Chem., Int. Ed.* **2001**, *40*, 23, 4425−4428. (b) Würthner, F.; Thalacker, C.; Diele, S.; Tschierske, C. *Chem. Eur. J.* **2001**, *7*, 10, 2245−2253. (c) Würthner, F.; Thalacker, C.; Sautter, A.; Schärtl, W.; Ibach, W.; Hollricher, O. *Chem. Eur. J.* **2000**, *6* (21), 3871−3886. (d) Struijk, C. W.; Sieval, A. B.; Dakhorst, J. E. J.; van Dijk, M.; Kimkes, P.; Koehorst, R. B. M.; Donker, H.; Schaafsma, T. J.; Picken, S. J.; van de Craats, A. M.; Warman, J. M.; Zuilhof, H.; Sudhölter, E. J. R. *J. Am. Chem. Soc.* **2000**, *122*, 11057−11066.

(6) (a) Benning, S.; Kitzerow, H.-S.; Bock, H.; Achard, M.-F. *Liq. Cryst.* **2000**, *27*, 7, 901−906. (b) Benning, S.; Hassheider, T.; Keuker-Baumann, S.; Bock, H.; Della Sala, F.; Frauenheim, T.; Kitzerow, H.-S. *Liq. Cryst.* **2001**, *28*, 7, 1105−1113. (c) Seguy, I.; Jolinat, P.; Destruel, P.; Mamy, R.; Allouchi, H.; Courseille, C.; Cotrait, M.; Bock, H. *ChemPhysChem* **2001**, *2* (7), 448−452. (d) Seguy, I.; Destruel, P.; Bock, H. *Synth. Met.* **2000**, *111*−*112*, 15−18. (e) Hassheider, T.; Benning, S.; Kitzerow, H.-S.; Achard, M.-F.; Bock, H. *Angew. Chem., Int. Ed.* **2001**, *40*, 11, 2060−2063.

(7) Berlman, I. B. *Handbook of Fluorescence Spectra of Aromatic Molecules*; Academic Press: New York, 1971.

(8) Förster, T.; Kasper, K. *Z. Electrochem.* **1955**, *59*, 976−981.

(9) Seyfang, R.; Port, H.; Fischer, P.; Wolf, H. C. *J. Lumin.* **1992**, *51*, 197−208.

(10) de Halleux, V.; Calbert, J. P.; Brocorens, P.; Cornil, J.; Declerq, J. P.; Brédas, J. L.; Geerts, Y. *Adv. Funct. Mater.* **2004**, *14*, 649−659.

(11) Vde Halleux, V. Fluorescent Discotic Liquid Crystalline Materials based on Pyrene, Ph.D. Thesis, Université Libre de Bruxelles, Brussels, 2002.

(12) Schenning, A. P. H. J.; Fransen, M.; Meijer, E. W. *Macromol. Rapid Commun.* **2002**, *23*, 4, 266−270.

(13) Vollmann, H.; Becker M.; Corell, H.; Streeck, *Justus Liebigs Ann. Chem.* **1937**, *531*, 1−159.

(14) Sonogashira, K.; Tohda, Y.; Haghiara, N. *Tetrahedron Lett.* **1975**, *50*, 4467.

(15) (a) Kroon, J. M.; Koehorst, R. B. M.; van Dijk, M.; Sanders, G. M.; Sudhölter, E. J. R. *J. Mater. Chem.* **1997**, *7*, 615−624. (b) Boulignand, Y. *J. Phys.* (*Paris*) **1980**, *41*, 1307.

(16) Tschierske, C. *J. Mater. Chem.* **2001**, *11*, 2647−2671.

(17) Barberá, J.; Giménez, R.; Serrano, J. L. *Chem. Mater.* **2000**, *12*, 481−489 and references therein.

(18) Donnio, B.; Heinrich, B.; Allouchi, H.; Kain, J.; Diele, S.; Guillon, D.; Bruce, D. W. *J. Am. Chem. Soc.* **2004**, *126*, 15258−15268.

(19) Salvi, P. R.; Foggi, P.; Castellucci, E. *Chem. Phys. Lett.* **1983**, *98*, 206−211.

(20) Wang, B.-C.; Chang, J.-C.; Tso, H.-C.; Hsu, H.-F.; Cheng, C.-Y. *J. Mol. Struct.* (*THEOCHEM*) **2003**, *629*, 11.

(21) de Mello, J. C.; Wittmann, H. F.; Friend, R. H. *Adv. Mater.* **1997**, *9*, 230−232.

(22) (a) Grice A. W.; Bradley, D. D. C.; Bernius, M. T.; Inbasekaran, M.; Wu, W. W.; Woo, E. P. *Appl. Phys. Lett.* **1998**, *73*, 629−632. (b) Temperature-dependent measurements have confirmed a quantum of fluorescence above 50%; see: Ariu, M.; Lidzey, D. G.; Sims, M.; Cadby, A. J.; Lane, P. A.; Bradley, D. D. C. *J. Phys.*: *Condens. Matter.* **2002**, *14*, 9975−9986.

(23) Ho, P. K. H.; Kim, J. S.; Burroughes, J. H.; Becker, H.; Li, S. F. Y.; Brown, T. M.; Cacialli, F.; Friend, R. H. *Nature* **2000**, *404*, 481−484.

(24) Cornil, J.; dos Santos, D. A.; Crispin, X.; Silbey, R.; Brédas, J. L. *J. Am. Chem. Soc.* **1998**, *120*, 1289.

(25) Xie, Z.; Yang, B.; Li, F.; Cheng, G.; Liu, L.; Yang, G.; Xu, H.; Ye, L.; Hanif, M.; Liu, S.; Ma D.; Ma, Y. *J. Am. Chem. Soc.* **2005**, *127*, 14152.

(26) Birks, J. B. *Rep. Prog. Phys.* **1975**, *38*, 903−974 (see p 918).

(27) Gareis, T.; Köthe, O.; Daub, J. *Eur. J. Org. Chem.* **1998**, 1549.

(28) Lai, R. Y.; Fleming, J. J.; Merner, B. L.; Vermeij, R. J.; Bodwell, G. J.; Bard, A. J. *J. Phys. Chem. A* **2004**, *108*, 376.

(29) Benniston, A. C.; Harriman, A.; Lawrie, D. J.; Rostron, S. A. *Eur. J. Org. Chem.* **2004**, 2272.

(30) Ferguson, J. *J. Chem. Phys.* **1958**, *28* (5), 765.

(31) Warshel, A.; Huler, E. *Chem. Phys.* **1974**, *6*, 463.

(32) Gierschner, J.; Mack, H.-G.; Oelkrug, D.; Waldner, I.; Rau, H. *J. Phys. Chem. A* **2004**, *108*, 257.

(33) Gierschner, J.; Ehni, M.; Egelhaaf, H.-J.; Milián Medina, B.; Beljonne, D.; Benmansour, H.; Bazan, G. C. *J. Chem. Phys.* **2005**, *123*, 144914.

(34) Birks, J. B. The Photophysics of Aromatic Excimers. In *The Exciplex*; Gordon, M., Ware, W. R., Eds.; Academic Press: New York, 1975; p 39.

(35) Kleppinger, R.; Lillya, C. P.; Yang, C. *J. Am. Chem. Soc.* **1997**, *119*, 4097.

(36) Festag, R.; Kleppinger, R.; Soliman, M.; Wendorff, J. H.; Lattermann, G.; Staufer, G. *Liq. Cryst.* **1992**, *11*, 699.

(37) Dewar, M. J. S.; Zoebish, E. G.; Healy, E. F.; Stewart, J. J. P. *J. Am. Chem. Soc.* **1985**, *107*, 3902.

(38) Zerner, M. C. In *Reviews in Computational Chemistry*; Lipkowitz, K. B., Boyd, D. B., Eds.; VCH: New York, 1991; Vol. II, p 313.